ChemComm

Accepted Manuscript

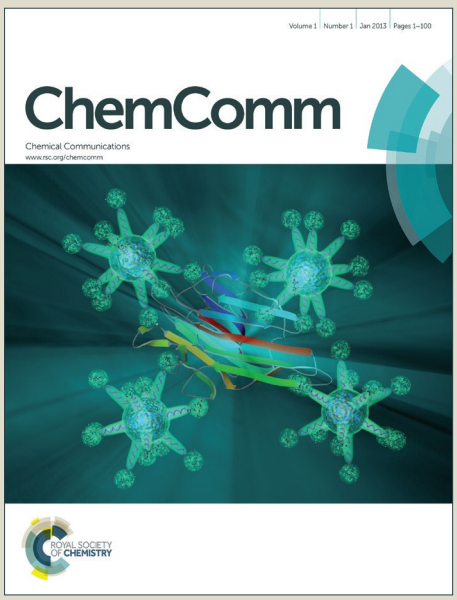

ROYAL SOCIETY OF CHEMISTRY

www.rsc.org/chemcomm

Journal Name

COMMUNICATION

Anomalous adsorption of biomolecules on a Zn-based metal-organic framework obtained via a facile room-temperature route

Received 00th January 20xx,
Accepted 00th January 20xx

DOI: 10.1039/x0xx00000x

www.rsc.org/

Alexandr V. Vinogradov*[a], Haldor Zaake-Hertling[b], Andrey S. Drozdov[a], Peter Lönnecke[b], Gulaim A. Seisenbaeva[c], Vadim G. Kessler[c], Vladimir V. Vinogradov[a] and Evamarie Hey-Hawkins*[b]

Here, we report a new method for crystal growth of two Zn-based MOFs at room temperature (known MOF-5 and a new modification of $[\{Zn_2(TBAPy)(H_2O)_2\}\cdot 3.5DEF]_n$ (1) employing slow diffusion conditions. Employing both Zn-based MOFs with different pore morphology made it possible to discover an anomalous adsorption of L-histidine in 1 of up to 24.3 × 10^{15} molecules cm^{-2} at 25 °C. This is one of the first reports aimed not only at describing a new method for targeted formation of crystalline MOFs and coordination polymers, but also at demonstrating the use of Zn-based MOFs as potential drug delivery materials, with the highly effective adsorption of L-histidine given here as an example.

Retaining high biological activity of biomolecules while delivering medicines is the main question to be answered by modern nanobiopharmaceuticals[1] science. The answers to this question are provided by several directions,[2, 3] each one being successfully established and having its own advantages and disadvantages.[3, 4] Among those most efficient are: 1) the synthesis of prodrugs (human enzymes convert a drug into an active compound),[5, 6, 7] 2) incorporation of a biologically active compound into a matrix system (microcapsules, microspheres, porous organic or inorganic structures, etc.),[8] and 3) binding of biomolecules to particles (altering the recognition of the compound by the human defense system)[9]. It is obvious that the most interesting materials would deal with several or all of the mentioned problems simultaneously. Biocompatible metal-organic frameworks (MOFs) are highly promising for this purpose.[3] Delivering biomolecules using MOFs can also prove superior due to the absence of the undesirable 'protein corona' effect which is observed at the nano–bio interface boundary.[10-12] It is due not only to the ordered arrangement of adsorption centers, but, first of all, to restricted mobility inside a microporous MOF that prevents coagulation and supramolecular self-assembly of biomolecules at the interface with high surface energy. Taking into account the huge difference in Arrhenius prefactor between native biomolecules and those entrapped in a nanoporous matrix,[13] one may highly appreciate the prospects of MOFs as potential drug delivery materials. The progress made to date includes examples of using MOFs as promising matrices for biomaterials.[14, 15, 16] Only in individual cases were anomalous adsorption values reached, usually related to the functionalization of the linkers in the MOFs with amino groups.[16]

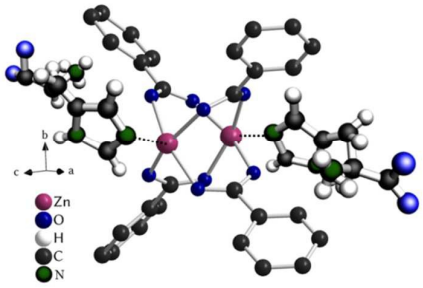

Figure 1. Visualization of a possible interaction between L-histidine and the secondary building unit (SBU, phenylene rings also included) in $[Zn_2(TBAPy)]_n$.

In this work, we have employed known[17] and novel Zn-based MOFs with different pore morphology since the simplest way of binding biomolecules is complexation with the Zn ions (Zn^{2+}). Due to this, the understanding of adsorption processes of for example proteins should start at the amino acid level, to enable predictions of possible conformations in the more complex protein structures.[18-22] As a result, this work deals with adsorption studies of the amino acid L-histidine, which possesses a high affinity to Zn^{2+} (Fig. 1).[23]

Additionally, the neutral imidazole ring of histidine can undergo tautomerization with ring flips (rotamerization) to interconvert between protonated and deprotonated forms with negligible changes in the space occupied by the ring, which is generally important for protein function[24]. Furthermore, L-histidine is known to coordinate effectively to

[a] ITMO University, St. Petersburg, 197101,Russian Federation.
[b]Leipzig University, Faculty of Chemistry and Mineralogy, Institute of Inorganic Chemistry, D-04103 Leipzig, Germany
[c]Department of Chemistry, BioCenter, Swedish University of Agricultural Sciences, Box 7015, 75007 Uppsala, Sweden.
† Electronic Supplementary Information (ESI) available: See DOI: 10.1039/b000000x/

transition metal ions in solution. These structural and chemical properties of histidine are utilized by biological systems, and as a result this amino acid is found in a large number of metalloproteins, ion channels, and enzyme active sites.[24] It is also a precursor of histamine, a biogenic amine that triggers local immune responses.[24-27]

However, one has to keep in mind that anomalous adsorption conditions will be attained in the cases when the number of adsorption centers (Zn^{2+}) is equal to the number of L-histidine molecules and the possibility of interactions between them is close to 100%. In this case, the pore morphology and possibility of free transport are important factors. Thus, the present work utilizes Zn-based MOFs with different pore morphology. The crystallization of Zn-based MOFs is mostly performed at room temperature, allowing future entrapment of biomolecules directly during the crystal growth process. The new method for crystal growth reported here using MOFs as an example can readily be applied to the other samples, including those requiring an inert atmosphere. For this, we used a new cell with the separation of the solution of the ligand and metal ions through the gas layer. The movement of gas through the capillary starts the interaction of the separated components by "suction" of the solution from vessel 3 to vessel 2, fig.2. This motion gradient is initiated by adiabatic compression of the gas in sphere 1, Figure 2, which is connected to vessel 2 *via* the capillary.

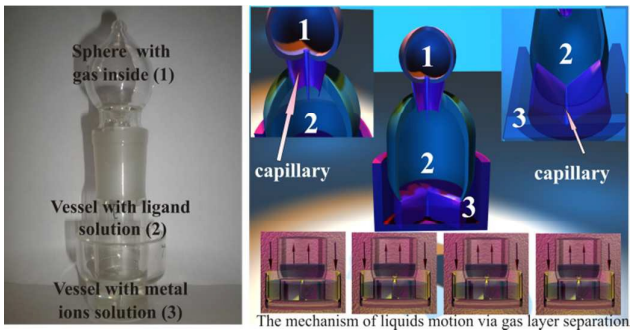

Figure 2. General view of a device that implements the proposed mechanism of crystal growth.

Using this method we facilitated way to crystals grow at room temperature. The crystal size was similar to what has been previously achieved. However, the advantage of this new method lies primarily in the fact that the recovery of the crystals becomes more convenient with crystals with best shapes and monodispersity.

A new room-temperature route for crystal growth of MOFs

Crystals of MOF-5[28] and $[\{Zn_2(TBAPy)(H_2O)_2\}\cdot 3.5DEF]_n$ (**1**) (TBAPy = 1,3,6,8-tetrakis(*p*-benzoate)pyrene) were obtained using a new method based on slow diffusion conditions created by the flow gradient in liquids separated by a gas layer (represented in ESI). Solvent removal was carried out in a vacuum degasser for MOF-5 [28, 31, 32] at 100 °C and for **1** at 220 °C during of 24 hours, forming the respective solvent-free crystals $[Zn_4O(O_2C\text{-}C_6H_4\text{-}CO_2)_3]_n$ (**2**) and $[Zn_2(TBAPy)]_n$ (**3**), respectively.

Preparation of biocomposites His@MOF was carried out by adsorption of the L-histidine from aqueous media. It is well known that zinc(II) forms strong complexes with L-histidine in common biological systems. Complexation constants[29] and energy (ΔG)[30] of zinc(II)-histidine significantly exceeds the zinc(II)-aqua complex. To this end, dried crystals of MOF-5 and **1** (5 g/L) (compounds **2** and **3**) were added to an L-histidine solution (0.5 mM) in $H_2O$and mixed for 20 min to achieve the adsorption equilibrium.

Nanomaterial Characterization. Here, a known pyrene-based ligand decorated with benzoic acid (HTBAPy = 1,3,6,8-tetrakis(*p*-benzoic acid)pyrene)[17,33] was employed. A Zn-based MOF with this linker was previously prepared hydrothermally ($([Zn_2(TBAPy)(H_2O)_2\cdot(Guests)]_n$),[17] while the room-temperature synthesis employed here results in a different modification of $[Zn_2(TBAPy)(H_2O)_2]_n$ (space group $I\bar{4}$[this work] vs. $P2/m$[17]).

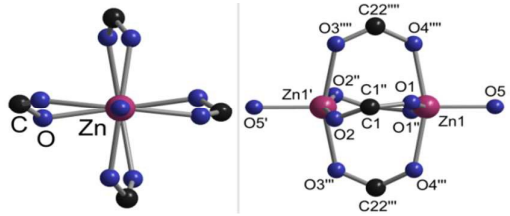

Figure 3. The new SBU front and side observed for $[\{Zn_2(TBAPy)(H_2O)_2\}\cdot 3.5DEF]_n$. The second Zn atom of the paddle wheel is symmetry- generated.

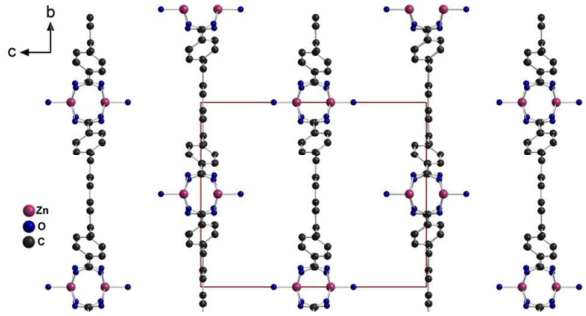

Figure 4. Layer structure of $[Zn_2(TBAPy)(H_2O)_2)\cdot 3.5DEF]_n$. Atoms are generated only by applying the symmetry operators [x,y,z] and [-x,-y,z]. Disordered atoms (symmetry operators [y,-x,-z] and [-y,x,-z]) and hydrogen atoms are omitted for clarity.

The structure that was obtained is similar to the structure published earlier;[17] however, the stacking is different and the SBUs are positioned more closely to each other. The SBU shows an often observed paddle wheel structure with a (non-bonding) Zn···Zn distance of 2.890(2) Å and Zn–$O_{carboxylate}$) bond lengths in the range of 2.006(1) Å to 2.078(1) Å and 1.937(6) Å for the Zn–O bond of the water molecules that are positioned on the wheel's Zn1···Zn1' axis, Fig. 3. The distance between adjacent layers in **1** (Fig. 3) is about 9.6 Å whereas the layers are closer in the already known structure (4.5 to 4.8 Å)[17]. The separation d of the layers can be expressed by d = c/2 as demonstrated in Figure 4. Taking these values into account, one may assume that these compounds are capable of transporting L-histidine molecules, in contrast to MOFs of the MOF-5 family, due to their unique structure and huge porosity. The phenyl rings are rotated with respect to the central pyrene

core by ca. 66.7° and 66.2° (diagonally opposite rings have the same angle).

The pore structure is visible in the direction along the *c* axis; there are 2 different pores, Fig. 5 and S10, with dimensions 7 Å x 11.3 Å and 13 Å x 9.1 Å for pores 1 and 2, respectively. The pores are filled with 3.5 highly disordered diethylformamide (DEF) molecules per formula unit.

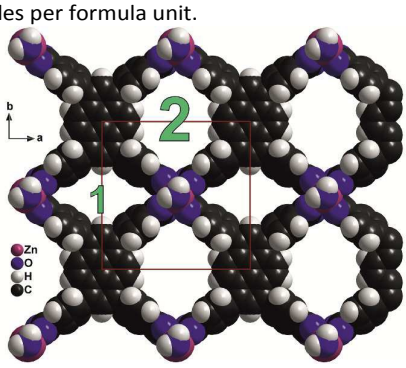

Figure 5. Pores in $[\{Zn_2(TBAPy)(H_2O)_2\}\cdot 3.5DEF]_n$ (**1**) (view along the *c* axis, space-filling model, hydrogen atoms, solvent molecules, and disordered ligands omitted for clarity).

In order to estimate the thermal stability of $[\{Zn_2(TBAPy)(H_2O)_2\}\cdot 3.5DEF]_n$ (**1**), thermal analysis (TG) was carried out in the range 25–600 °C. After removal of water and DEF molecules (at 125 °C and 230 °C, respectively), the $Zn_2(TBAPy)$ framework is stable up to 415 °C (Fig. S8 in ESI). This thermal behavior stability is comparable to that of an already known Zn-based MOF.[17] The permanent porosity of the dried (activated) sample ($[Zn_2(TBAPy)]_n$) was confirmed by N_2 sorption isotherms at 77 K (Fig. S9 in ESI). The BET and Langmuir surface areas are 615 and 784 m^2g^{-1}, respectively, which were calculated using the adsorption data in the relative pressure range p/p_0 = 0.06–0.3. The total pore volume of $[Zn_2(TBAPy)]_n$ is 0.245 cm^3/g, and the pore radius (Dubinin–Astakhov (DA)) is 0.69 nm.

Comparing the simulated structure concept with HRTEM of single crystals, Fig. 6C, we developed an arbitrary axis of a sub-micrometer sized single crystal. The habitus of the crystals is square planar, which is in excellent correlation with the observed tetragonal structure and the formation of layers in the *a-b* plane which are connected only by weak van-der-Waals interactions in the *c* direction. HRTEM experiments were carried out with a very low electron dose level, but the crystal was still damaged during the alignment. One of the HRTEM images is shown in Fig. 6b. Evidence of a highly porous structure is also provided by HRTEM (Fig. 6c), in full agreement with the structural data obtained using single-crystal X-ray diffraction. The high resolution images demonstrate a long-range ordered structure of $[\{Zn_2(TBAPy)(H_2O)_2\}\cdot 3.5DEF]_n$ (**1**). The peculiarity of this layered structure is the main difference from previous experiments carried out for an analogous compound.[17] The interplanar distance of ca. 1.1 nm (according to the HRTEM data) is in excellent correlation with the X-ray crystal structure and supports the idea of forming open cylindrical pores (Fig. 5), promoting efficient transport of molecules complementary to this structure, which is observed for L-histidine.

Another important confirmation of histidine sorption in the process of coordinative interaction with the Zn^{2+} ions is fluorescence. It was shown previously[17] that crystalline $[Zn_2(TBAPy)]_n$ exhibits extremely strong fluorescence, in contrast to the MOF-5 family.[34] The specific fluorescence of L-histidine upon complex formation with metals is used as a biosensor detection method.[35,36] Here, this method was also employed to assess the prospects of **3** as biosensor (Fig. S11). The IR spectroscopic data (Fig. S4 in ESI) have shown that adsorption of L-histidine on crystalline $[Zn_2(TBAPy)]_n$ is due to interaction with the imidazole group, which is a unique feature of the system and may be promising for future sensorics and separation of L-histidine/ L-cysteine by fluorescence investigation,[35] which often find application as a test system to distinguish histidine from other imidazole derivatives.[37,38] In addition, this fluorescent sensor can also distinguish histidine from other imidazole derivatives. In this study we have performed a comparative analysis of 3D fluorescence spectra of pure $[Zn_2(TBAPy)]_n$ (**3**) (Fig. S11B), pure L-histidine (Fig. S11D), and L-histidine@$[Zn_2(TBAPy)]_n$ (Fig. S11C). It turned out that **3** can serve as a highly selective fluorescent sensor for L-histidine. The fluorescence enhancement in the presence of L-histidine was accompanied by an excitation wavelength shift with a maximum at 545 nm (in contrast to 320 nm for **3** and 390 nm for L-histidine) and a substantial increase in intensity. The absence of fluorescence in the solution after centrifugation and separation of the liquid fraction can also be considered as evidence of L-histidine interaction with **3**. In contrast, no similar changes were found when **2** was

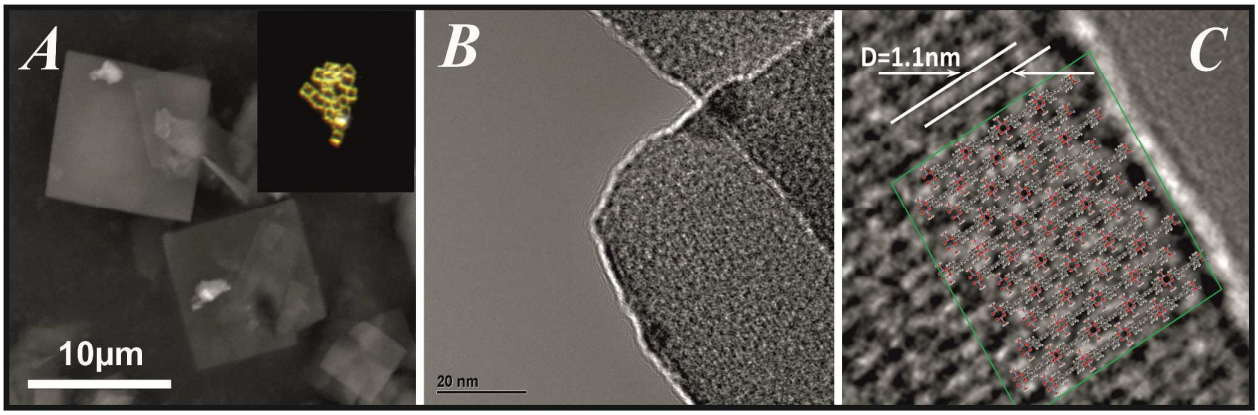

Figure 6. a) SEM and optical image (as insert), b) HRTEM and c) a thin boundary selected from (b) with impregnated MOF structure images of $[Zn_2(TBAPy)]_n$ (**3**).

employed. In MOF-5, all Zn cations are coordinatively saturated and therefore no interaction with any donors, such as imidazol, would be possible. This also supports the assumption that the effect is indeed due to Zn-imidazole interaction. Adsorption of L-histidine on the surface as MOFs porous structure also obtained *via* low-temperature N_2 physisorption. We've detected that surface area and pore DA radii decreasing for both samples accordingly the L-histidine presence, table S1 (detail in ESI). Probably, reducing surface area on MOF-5 is likely due to the influence of water molecules on the structure of MOF, as reported before [31], despite the fact that it is reproduced PXRD data. Quantitative assessment of L-histidine adsorption on crystalline **2** and **3** was carried out using UV-vis spectroscopic investigations at 28 °C (Fig. S5 in ESI). The data revealed the sorption values to be 4.8 × 10^{15} molecules·cm^{-2} for MOF-5 and a five times higher value of 24.3 × 10^{15} molecules·cm^{-2} for **3** for a 2-day exposure. The presence of a layered structure in **3** with an increased pore radius is likely to promote an increase in L-histidine adsorption due to coordinative interactions. These results are also supported by no change in zeta potential for **3** in the presence of L-histidine (Fig. S9 in ESI). Based on these results, one may conclude that sorption of L-histidine is not related to electrostatic or coagulation interactions between amino acid molecules and MOF particles. Thus, the inferences on chemical coordination are found and confirmed by fluorescence and IR spectroscopy.

It is quite known that MOFs are sensitive to hydrolysis and the stability of MOF-5 in water is poor. Stability assessment derived MOFs assessed by PXRD, Fig.S6, S7. The both compounds MOF-5 and ***3*** possess a high stability in aqueous solutions.

Finally, this work describes a new simple room-temperature method of forming crystals of MOFs and coordination polymers as demonstrated by the synthesis of already known (MOF-5) and new (1) compounds. It is shown that $[\{Zn_2(TBAPy)(H_2O)_2\}\cdot 3.5DEF]_n$, after elimination of water and DEF molecules, exhibits a unique capability to absorb L-histidine by coordination via imidazole at the zinc ion in contrast to MOF-5 (five times lower). A special layered structure is likely to provide transport of L-histidine molecules while retaining high mobility. This effect of L-histidine sorption resulted in extremely strong fluorescence, revealing the possibility to use this compound as a biosensor for amino acids and possibly also small peptides containing imidazole groups. The properties discovered here open the door to new promising branches of applying and using MOFs and coordination polymers.

This work was supported by the Russian Government, Ministry of Education and by the RFBR, Research Project No.14-03-31046. Alexandr Vinogradov would like to thank the German Academic Exchange Service (DAAD) for financial support.

Notes and references

1. M.Veerapandian, M. Marimuthu, K.-S. Yun, S. Kim *Thai J. Pharm. Sci.*, 2009, **33**, 1.
2. F. Fenaroli, D. Westmoreland, J. Benjaminsen, T. Kolstad, F. M. Skjeldal, A.H. Meijer, M. van der Vaart, L. Ulanova, N. Roos, B. Nyström, J. Hildahl, G. Griffiths *ACS Nano*, 2014, **8**, 7014.
3. T. Faust *Nature Chemistry*, 2015, **7**, 270.
4. C. Harrison *Nature Reviews Drug Discovery*, 2013, **12**, 24
5. D. Reimer, K. M. Pos, M. Thines, P. Grün, H. B Bode *Nat Chem Biol*. 2011, **7**, 888.
6. L.F. Tietze, K. Schmuck, H.J. Schuster, M. Müller, I., Schuberth *Chemistry*, 2011, **17**, 1922.
7. X.-T.Liang, W.-S. Fang, Medicinal Chemistry of Bioactive Natural Products John Wiley & Sons, 2006**.**
8. a) V.V. Vinogradov, D. Avnir *RSC Advances* 2015, **5**, 10862. b) A.V. Vinogradov, V.V. Vinogradov, *RSC Advances* 2014**, 4**, 45903.
9. M. Konerackáa, P. Kopcanský, M. Timko, C.N. Ramchand, A. de Sequeira, M. Trevan *Journal of Molecular Catalysis B: Enzymatic, 2002,* **18**, 13.
10. A. A. Shemetov, I. Nabiev, A. Sukhanova, *ACS Nano*, 2012, **6**, 4585.
11. J. E. Gagner, S. Shrivastava, X. Qian, J.S. Dordick R.W. Siegel *J. Phys. Chem. Lett.* 2012, **3**, 3149.
12. A. Vallee, V. Humblot, C.-M. Pradier, *Acc. Chem. Res* 2010, **43**, 1297.
13. V.V. Vinogradov, D. Avnir *Journal of Material Chemistry B*, 2014, **2**(19) 2868.
14. P. Horcajada, C.Serre, G.Maurin, N. A. Ramsahye, F. Balas, M., Vallet-Regí, M. Sebban, F.Taulelle, G. Férey *J. Am. Chem. Soc.*, 2008, **130** (21), 6774.
15. R.C. Huxford, J.D. Rocca, W. Lin, *Curr. Opin. Chem. Biol.* 2010, **14**(2), 262–268.
16. P. Horcajada, et al., *Nature Materials* 2010, **9**, 172.
17. K. C. Stylianou, *J. Am. Chem. Soc.* 2012, **134**, 20466.
18. J. Schaefer, C. Schulze, E.E.J. Marxer, U.F. Schaefer, W. Wohlleben, U. Bakowsky, C.-M. Lehr *ACS Nano* 2012**, 6**, 4603.
19. K. Prapainop, D.P. Witter, P. Wentworth *J. Am. Chem. Soc.*, 2012, **134** (9), 4100.
20. R. Podila, P. Vedantam, P. C. Ke, J. M. Brown, A. M., Rao, *J. Phys. Chem. C* 2012, **116**, 22098.
21. A. Rimola, Y. Sakhno, L. Bertinetti, M. Lelli, G. Martra, P. Ugliengo *J. Phys.Chem. Lett.* 2011, **2**, 1390.
22. A. Rimola, M. Corno, M. Zicovich-Wilson, P. *J. Am. Chem. Soc.* 2008, **130**, 16181.
23. L. Zhou, S. Li, Y. Su, X. Yi, A. Zheng, F. Deng *J. Phys. Chem. B*, 2013, **117** (30) 8954.
24. I. A., Mudunkotuwa, V. H., *Langmuir*, 2014, **30**, 8751.
25. Li S. Hong M. *J. Am. Chem. Soc*. 2011, **133**, 1534.
26. V. Feyer, O. Plekan, T.S. Skala, V.R. Chab, V.R. Matolín, K.C.Prince, *J. Phys. Chem. B,* 2008, **112**, 13655.
27. P.R. Reddy, M. Radhika, P. Manjula *J. Chem. Sci.,* **117**(3), 2005, 239.
28. O.M. Yaghi, H. Li, *J. Am. Chem. Soc.,* 1995, **117**, 10401.
29. T., Dudev, C., Lim. *J. Am. Chem. Soc.*, 2000, **122** (45), 11146.
30. Y. Altun, F.Köseoğlu *J. Sol. Chemistry*, 2005, **34** (2), 213.
31. R. Custelcean, M.G. Gorbunova; *J. Am. Chem. Soc.*, 2005, **127** (47), 16362.
32. P.V. Dau, K.K., Tanabe, S.M. Cohen *Chem. Comm.,* 2012, **48**, 9370.
33. R.-J. Li, M. Li, X.-P. Zhou, D. Li M. O'Keeffe Chem. Comm, 2014, **50**, 4047.
34. V. Halleux, J.-P. Calbert, P. Brocorens, J. Cornil, J.-P. Declercq, J.-L. Brédas, Y. Geerts, *Adv. Functional Materials,* 2004,**14**-7, 649.
35. J. Du, Z. Huang, X.-Q., Yu L. Pu, *Chem. Commun.,* 2013, **49**, 5399.
36. M. A. Hortala, L. Fabbrizzi, N. Marcotte, F. Stomeo *J. Am. Chem. Soc.*, 2003, **125**, 20.
37. K.L. Haas, A.B. Putterman, D.R. White, D. J. Thiele, and K.J. Franz, *J. Am. Chem. Soc.*, 2011, **133**, 4427.
38. J.D. Galpin, B.E. Ellis, and M. E. Tanner *J. Am. Chem. Soc.*, 1999, **121**, 10840.